A Letters Journal Exploring the Frontiers of Physics

April 2018

EPL, **122** (2018) 20003 www.epljournal.org
doi: 10.1209/0295-5075/122/20003

Mesoscopic modelling of microbubble in liquid with finite density ratio of gas to liquid

Dingyi Pan, Gengyao Zhao, Yuqing Lin[a] and Xueming Shao

State Key Laboratory of Fluid Power and Mechatronic Systems, and Key Laboratory of Soft Machines and Smart Devices of Zhejiang Province, Department of Engineering Mechanics, Zhejiang University - Hangzhou 310027, China

received 5 February 2018; accepted in final form 22 May 2018
published online 18 June 2018

PACS 02.70.Ns – Molecular dynamics and particle methods
PACS 47.11.-j – Computational methods in fluid dynamics
PACS 68.03.-g – Gas-liquid and vacuum-liquid interfaces

Abstract – A microbubble model is developed with the mesoscopic simulation tool, dissipative particle dynamics (DPD) and many-body dissipative particle dynamics (MDPD). Standard DPD particles are employed to represent bubble phase at low density, and MDPD particles are for the liquid phase. The microbubble can be stable in liquid, in contrast to the vacuum bubble model. Gas-liquid interface is well presented with density and pressure jumps. The density ratio of gas to liquid can be lower than 0.1 by increasing the cut-off radius of bubble particles. Oscillating behavior of the microbubble model is investigated and validated by comparing with the Rayleigh-Plesset equation. The current model shows correct dynamic response, and the fluctuating behavior is captured as well. The lower the density ratio of the microbubble model, the closer the oscillating frequency to that of continuum theory.

Introduction. – Microbubble is an important matter for scientific research which is ubiquitous in nature and in industry [1]. Microbubble acts as the nuclei for the inception of cavitation [2], which is harmful, making noise and causing structure damage of the propeller. In biomedical engineering, ultrasonic driven microbubble has been used to enhance contrast in ultrasonic images, noninvasive therapy and drug delivery with sonoporation [3,4]. Studies on bubble and microbubble dynamics have been widely reported in last two decades. Concerning cavitation inception, researches mainly focus on growth and oscillation of microbubble (cavitation nuclei) with ten to hundred microns in diameter, and consequent collapse. A set of microbubbles with specific size distribution is released in the fluid coupled with certain flow pattern [5], *e.g.*, vortex flow, and bubble dynamics can be described by the well-known Rayleigh-Plesset (RP) equation [6]. While the dynamic behavior of smaller bubbles, *i.e.*, homogeneous cavitation [7], has not been paid enough attention to. On the other hand, the so-called nanobubbles have been observed recently in laboratory, either on solid surface or in bulk fluid [8]. The Laplace pressure of bubbles in such small scale is quite high from a theoretical estimation, and the stability of these nanobubbles has not been comprehensively explained.

The aforementioned microbubbles are in the length scale from ten nanometers to several microns. The classical continuum theory may not be able to fully capture the fluctuation phenomenon in microscale, and meanwhile, the interactions of gas, liquid and solid phases are difficult to define. Therefore, a bottom-up microbubble model is necessary for the study in those areas. The molecular dynamics (MD) simulation could be a reliable approach for the modelling of microbubble. It is also straightforward in the modelling of biological membranes and cells, extending to the study in bubble-membrane/cell interactions. However, due to its small length and time scales, the current MD simulation is only applicable for a simulation box in several nanometers in 10 to 100 nanoseconds [9]. The coarse-grained MD simulations or mesoscopic simulation tools are one of the solutions that may extend the simulation size and period. In this work, we are aiming to create a mesoscale microbubble model which may be applied in the study of microbubbles in larger length and longer time scales. The mesoscale simulation tool, dissipative particle dynamics (DPD), is used to construct the current microbubble model. Moreover, the classical theory of bubble dynamics is employed to validate the model.

[a]E-mail: linyuqing@zju.edu.cn

Simulation tools. – The original DPD method was introduced by Hoogerbrugge and Koelman [10]. It is considered as one of the coarse-grained approaches of MD simulation. The governing equations in DPD are Newton's second laws of motion. For particle i, the governing equations are given by $\mathbf{f}_i = \mathrm{d}\mathbf{v}_i/\mathrm{d}t$, where $\mathbf{f}_i$ is the summation of inter-particle forces exerted by all the other particles. Español and Warren [11] suggested that the inter-particle force $\mathbf{f}_i$ can be decomposed into three pairwise and centre-to-centre forces, *i.e.*, conservative force, dissipative force and random force, as $\mathbf{f}_i = \sum_{j\neq i}(\mathbf{F}_{ij}^C + \mathbf{F}_{ij}^D + \mathbf{F}_{ij}^R)$. In particular, a soft repulsive potential is employed, and the conservative force can be written as

$$\mathbf{F}_{ij}^C = a_{ij} w_C(r_{ij}) \widehat{\mathbf{r}}_{ij}, \tag{1}$$

where a_{ij} is the amplitude, w^C the weight function and $\widehat{\mathbf{r}}_{ij} = \mathbf{r}_{ij}/r_{ij}$. In conventional DPD, this conservative force only linearly depends on the inter-particle separation, and therefore, it is not able to exhibit vapor-liquid coexistence and phase transition. Thereafter, the many-body dissipative particle dynamics (MDPD) was developed aiming to construct a non-ideal fluid system [12]. In MDPD, the conservative force is a density-dependent function, and the van der Waals loop is therefore created. The conservative force of MDPD proposed by Warren [13] is

$$\mathbf{F}_{ij}^C = [A_{ij} w_C(r_{ij}) + B_{ij}(\bar{\rho}_i + \bar{\rho}_j) w_d(r_{ij})]\widehat{\mathbf{r}}_{ij}. \tag{2}$$

It consists of two parts: a density-independent attractive force ($A_{ij} < 0$), which is similar to standard DPD conservative force, only depending on the inter-particle separation, and a repulsive force ($B_{ij} > 0$) depending on the instantaneous local density [14]. Here, $\bar{\rho}_i$ and $\bar{\rho}_j$ are the local instantaneous density on the position of particle i and j. Moreover, this two-parts conservative force has different cut-off radii r_C and r_d for the weight functions w_C and w_d, respectively. In addition, the dissipative force and random force consist in a thermostat by fulfilling the fluctuation-dissipation theorem, and the system temperature can be kept as constant. Both DPD and MDPD share the same formations of these two forces:

$$\mathbf{F}_{ij}^D = -\gamma w^D(r_{ij})(\widehat{\mathbf{r}}_{ij}\cdot\mathbf{v}_{ij})\widehat{\mathbf{r}}_{ij}, \quad \mathbf{F}_{ij}^R = \sigma w^R(r_{ij})\theta_{ij}\widehat{\mathbf{r}}_{ij}. \tag{3}$$

Here γ and σ are the amplitudes, $\mathbf{v}_{ij}$ the relative velocity and θ_{ij} is a randomly fluctuating variable with Gaussian statistics which satisfies $\langle\theta_{ij}\rangle = 0$ and $\langle\theta_{ij}(t)\theta_{kl}(t')\rangle = (\delta_{ik}\delta_{jl} + \delta_{il}\delta_{jk})\delta(t-t')$. w^D and w^R are the weight functions which are short-ranged that all these forces vanish at $r_{ij} \geq r_c$.

The original DPD method, as a quite successful mesoscale method to mimic hydrodynamics, is still not flexible enough to simulate the accurate thermodynamic behavior of a real system. The most substantial reason is that the DPD fluid produces an equation of state (EoS) which is different from the one of a real fluid. The approximated EoS of a DPD fluid is given by the following equation ($r_C = 1.0$) [15]:

$$p = \rho k_B T + \alpha a \rho^2 \ (\alpha = 0.101 \pm 0.001), \tag{4}$$

where p and ρ are the pressure and the number density of the DPD particles in DPD units, a is the repulsive strength which is equal to a_{ij} for all particle pairs in a single-component system, and α is a fitting parameter in DPD reduced units. For $\rho \geqslant 2$ and $a \geqslant 15$, it would be a good approximation as verified by Groot and Warren [15]. This DPD EoS has rigid quadratic density dependence irrespective to the parameter values [14]. Comparing the original DPD, the MDPD method adopts a different definition of the conservative force. Consequently, it produces a different EoS, which is given by Warren [13] fitting with the simulation data

$$p = \rho k_B T + \alpha A \rho^2 + 2\alpha B r_d^4(\rho^3 - c\rho^2 + d), \tag{5}$$

where $A(<0)$ and $B(>0)$ is the attractive and repulsive strength, and α, c and d are fitting parameters, which are equal to 0.101 ± 0.001, 4.16 ± 0.02 and 18 ± 1, respectively. The EoS contains a van der Waals loop which is able to construct vapor-liquid coexistence.

Microbubble model. – For a stable bubble, the well-known Young-Laplace equation describes the balance on the gas-liquid interface, which is

$$\Delta p = \gamma\left(\frac{1}{R_1} + \frac{1}{R_2}\right), \tag{6}$$

where Δp is the pressure difference across the gas-liquid interface, γ is the surface tension and R_1 and R_2 are the principle radii of local curvature. In the past, the vacuum bubble models in micro or mesoscale were employed [16,17], which are one of the simplest bubble models with gas-to-liquid density ratio equal to zero. The vacuum bubble is empty without any particle or molecule to be included. Therefore, the bubble will collapse due to the effects of the outside bulk liquid pressure and surface tension. Moreover, the vacuum bubble is not able to capture its dynamic behavior as well. Recently, Tran-Duc *et al.* [18] introduced the so-called hard-core bubble model in DPD simulation, which is a development of the single DPD model proposed by Pan *et al.* [19]. In detail, one single DPD particle with exponential shaped potential is used to represent the bubble, and the dissipative coefficient is adjusted to yield the correct hydrodynamic behavior of a single bubble. This model simplifies the treatment around the gas-liquid interface and also reduces the computation time consumption. However, it is only applicable for a spherical bubble due to the nature of the single-particle approach. An alternative approach for considering bubble deformation and its dynamic behavior is to follow the strategies of simulating a droplet with DPD [20,21], *i.e.*, two sets of DPD particles are employed to represent the droplet/bubble and solvent liquid, respectively. Normally, only the equal density

situation across the liquid-liquid interface is considered, whereas in bubble modelling, both the density jump (density ratio) and pressure jump across the interface as well as the compressibility of gas phase are key features, which should be carefully captured. The density ratio might be achieved by tuning the particle mass in bubble area coupling with a special numerical algorithm for small mass (stiff) system [22]. However, these would cause that the solvent liquid particle and bubble particle are in different coarse-graining levels, and subsequently the momentum exchange across the interface is hard to define.

To address the concerns mentioned above, we propose a new microbubble model in DPD, which can capture both the density and pressure jumps across the gas-liquid interface properly, and meanwhile yield the correct dynamic behavior for both stable and non-equilibrium microbubbles. In general, the MDPD particle and DPD particle are used to represent the liquid phase and gas phase (bubble), respectively. In particular, considering a stable convex bubble with positive surface tension pointing into the bubble area, the local balance from eq. (6) requires the pressure difference across the gas-liquid interface to be $p_{out} < p_{in}$, where p_{out} is the solvent pressure outside the bubble and p_{in} is the pressure inside the bubble. Moreover, the density jump requires $\rho_{out} > \rho_{in}$. The proportional dependence of pressure to density in eq. (4) of the original DPD EoS is not able to fulfill these two relationships. On the other hand, the MDPD EoS in eq. (5) is able to produce a state with lower density and larger pressure, however, our previous numerical simulation shows that the particle distribution is no longer homogeneous once the globe density is lower than a certain value [23]. Therefore, it is not feasible to construct the microbubble model with one single kind of particle species, neither original DPD nor MDPD. Instead, the combined DPD and MDPD model becomes a compromising choice. In fact, the current model can benefit from both advantages of DPD and MDPD. First, using a MDPD particle to represent the liquid phase, its van der Waals EoS is more realistic and moreover it presents a sharp interface [13]. Second, the Schmidt number of a DPD fluid is quite low, which is more a gas than a liquid [24], and moreover, the number density of the bubble phase in the current model is around 1 or less than 1, and the DPD fluid with number density around this value behaves like an ideal gas fluid, as shown in the EoS results [23].

In the current simulation, a cube of liquid particles is first generated and a sphere void is cut out from the centre of the cube. A sphere of bubble particles with lower density is then generated and the cube void is filled with this sphere. After then, the system is run 5000 time steps to achieve an equilibrium state. The particle number of liquid phase is around 560000 and the particle number of the bubble phase is 528. The outside liquid pressure is kept constant and the system is working in a NPT. The parameters are shown in table 1. The conservative forces of bubble and liquid particles are all in the same form of eq. (2), and the MDPD potential would be reverted back to the original DPD potential when $A_{ij} > 0$ and $B_{ij} = 0$. A large repulsive force is imposed on the bubble-to-liquid interaction to produce the surface tension. In the following, only the DPD units are employed. As a coarse-grained method, the correlation between DPD units and real physical units can be obtained through previous work of Ghoufi and Malfreyt [25,26]. Figure 1 shows the particle distributions in a slice of the computation domain of current microbubble model at different instances. For comparison, the results of vacuum bubble model are also given. It is clearly shown that the vacuum bubble shrinks once the computation starts and finally collapses when $t^* = 30$ in DPD unit, whereas the gaseous bubble turns to be stable from $t^* = 0$ to $t^* = 110$. The particles in gaseous phase have a relative lower number density than those in liquid phase. In addition, both the vacuum bubble and gaseous bubble have sharp boundaries at the interfaces.

Table 1: Parameters in the current simulation of a microbubble in liquid. LL: liquid and liquid particles, BB: bubble and bubble particles, BL: bubble and liquid particles. Other parameters in the current simulation are fixed as: dissipative coefficient $\gamma = 4.5$, Boltzmann temperature $k_BT = 1.0$.

	A_{ij}	B_{ij}	r_C	r_d
LL	−40	25	1.0	0.75
BB	25	0	1.0–1.6	N.A.
BL	25	0	1.0	N.A.

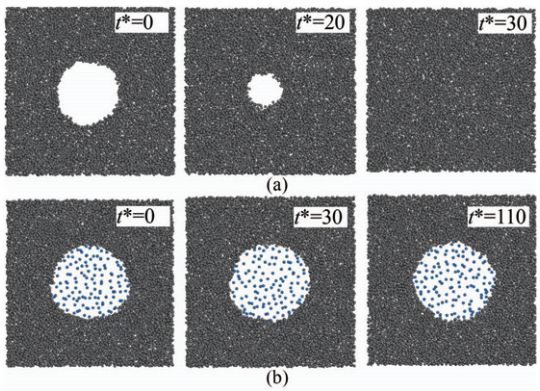

Fig. 1: (Colour online) Slices of the computation domain at different instances (t^* is in DPD unit), (a) vacuum bubble, (b) gaseous bubble.

Gas-liquid interface. – In order to obtain a quantitative results of both density and pressure jumps across the gas-liquid interface, we further calculate the radial distribution densities of bubble particle and liquid particle with respect to the bubble centre, which is a modification of the radial distribution functions (RDF):

$$\rho(r) = \frac{\langle n \rangle}{\frac{4\pi}{3}[(r+\Delta r)^3 - r^3]} \approx \frac{\langle n \rangle}{4\pi r^2 \Delta r} \quad (\Delta r \ll 1), \qquad (7)$$

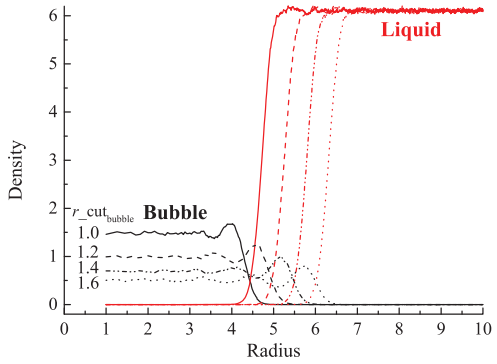

Fig. 2: (Colour online) Radial distribution function of particle densities with respect to the bubble centre, simulation parameters are given in table 1.

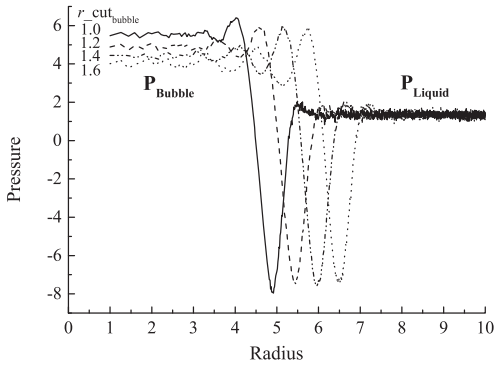

Fig. 3: Pressure distribution along the radial direction with respect to the bubble centre.

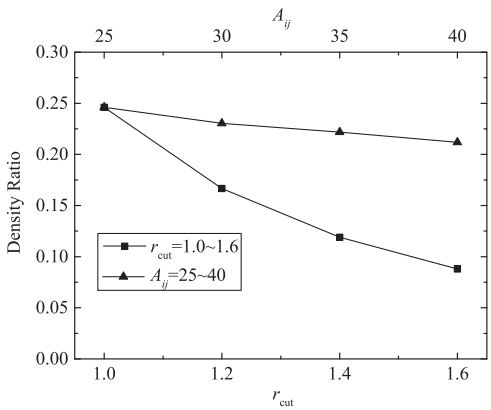

Fig. 4: Density ratios of bubble phase to liquid phase under changes of the cut-off radius for bubble particles and conservative-force amplitude for bubble particles.

where $\langle n \rangle$ is the particle number density in a spherical shell of width Δr at a radial distance from $r \to r + \Delta r$ with respect to the bubble centre. The approximation can be accepted when $\Delta r \ll 1$. The results of radial density is given in fig. 2, with cut-off radius of bubble particle ranging from 1.0 to 1.6. Density jumps are obtained in this figure, and there is no bubble particle entering into the bulk liquid phase and vice versa. The densities are almost uniform both in the bubble phase and the liquid phase. Therefore, a microbubble in liquid with finite density ratio is created in this simulation. For the calculation of bubble radius, we first derive the mean density of the bubble region from the RDF of gas particles density and then we obtain the bubble radius from total number of bubble particles and the mean density. In our simulation, no bubble particles enter into the bulk liquid region.

The pressure distributions/jumps along the radial direction with respect to the bubble centre are shown in fig. 3. The magnitudes of pressure are derived from the Irving-Kirkwood approach [27], and the outside liquid pressure is kept to be constant by the Berendsen barostat. The inside bubble pressure is a little larger than the outside liquid pressure to balance the effect of surface tension. We also capture the pressure fluctuations around the interface, which may be caused by the strong interactions between bubble particle and liquid particle, in detail, there is a transition region (finite width of interface) mixed with both bubble particles and liquid particles, particles are stretched in this region making them in a metastable state [28] and a similar phenomenon was also presented by MD simulation [29]. With the values of the inside and outside pressure, coupling with the Young-Laplace equation (eq. (6)), we can easily obtain the surface tension of the gas-liquid interface when the bubble is in its stable state.

To test the capability of the current model, we vary the magnitude of the parameters in DPD and MDPD to check their influence on the gas-to-liquid density ratio. Two major control parameters are investigated, *i.e.*, the cut-off radius for bubble particles and the amplitude of the conservative force for bubble particles. The results are given in fig. 4. It is shown that the cut-off radius of the bubble particle could be an effective parameter in tuning the density ratio, while the effect of conservative amplitude is relatively weak. As a preliminary test, the parameters are varied in a small range. With $r_C = 1.6$, we can achieve a gas-to-liquid density ratio lower than 0.1.

Microbubble dynamics. – From the viewpoint of application, the oscillating behavior of microbubbles plays a significant role [30]. In order to capture and validate the oscillating behavior of the current model, we first create a stable microbubble and then increase the outside pressure to drive the microbubble to oscillation. The partial Berendsen barostat [23] is used to keep the outside pressure constant and moreover without any artificial effect on the inside bubble. To quantitatively validate the current model, we borrow the theory of bubble dynamics from continuum theory. By investigating one single bubble dynamics in an infinite fluid field, Rayleigh [31] first derived the following equation:

$$\rho_l \left(R\ddot{R} + \frac{3}{2}\dot{R}^2 \right) = p_v - p_\infty, \tag{8}$$

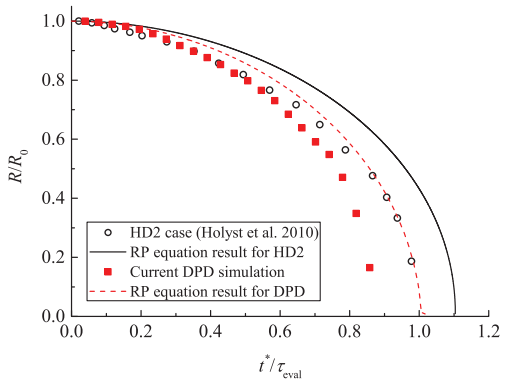

Fig. 5: (Colour online) Collapse of vacuum bubble, current DPD simulation (square symbol) and its comparison with previous MD simulation [33] (circle symbol) and solution of RP equation (lines). Parameters in DPD simulation and relevant RP equation are $P_\infty = 11.35$, $\mu = 5.58$, $\rho_l = 6.10$, $\sigma = 8.56$, $R(t_0) = 3.85$ and $\tau_{eval} = 2.56$. Parameters in MD simulation and relevant RP equation are $P_\infty = 0.9$, $\mu = 2.3$, $\rho_l = 0.825$, $\sigma = 0.67$, $R(t_0) = 25$ and $\tau_{eval} = 21.7$, all are in reduced units.

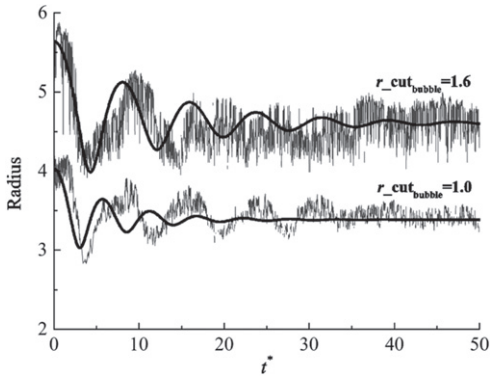

Fig. 6: Instantaneous bubble radius of oscillating bubble from DPD simulation (thin grey lines) and RP equation (thick black lines). Parameters for DPD simulation are the same as those in table 1. Parameters used for the solution of the RP equation are, upper line: $P_\infty = 11.35$, $\mu = 5.58$, $\rho_l = 6.10$, $\sigma = 7.57$ and $R(t_0) = 5.63$; lower line: $P_\infty = 11.35$, $\mu = 5.58$, $\rho_l = 6.10$, $\sigma = 8.56$ and $R(t_0) = 4.02$, all are in DPD units.

where ρ_l is the density of liquid, p_v and p_∞ are the vapor pressure and the liquid pressure in the far field, respectively, and R is the bubble radius. Later on, Plesset and Chapman [32] improved the Rayleigh equation by considering the liquid viscosity and surface tension. This is now the well-known RP equation:

$$\rho_l \left(R\ddot{R} + \frac{3}{2}\dot{R}^2 \right) = p_B - p_\infty - 4\mu\frac{\dot{R}}{R} - \frac{2\sigma}{R}, \qquad (9)$$

where μ is the liquid viscosity, σ is the surface tension and p_B represents the pressure inside the bubble. In deriving the above equations, the density ratio of bubble phase to liquid phase and the viscosity of the bubble phase were assumed to be zero. Therefore, there is no inertial effect and viscosity dissipation inside the bubble region. The bubble phase pressure is also prescribed, *e.g.*, for the vacuum bubble model, the bubble pressure (p_v in eq. (8) and p_B in eq. (9)) can be directly set to zero. For the comparison with our DPD results, eq. (9) is solved numerically with the 4th-order Runge-Kutta method. The liquid viscosity, surface tension and initial bubble radius are input from DPD results. The DPD EoS is also incorporated to obtain the value of p_B.

We first study the collapse of a vacuum bubble with the current DPD simulation. Hołyst *et al.* [33] used MD simulation to study the collapse of the vacuum bubble and later the collapse property triggered by a travelling wave [34]. The comparison with MD simulation (HD2 case in Hołyst *et al.* [33]) is shown in fig. 5. Both the instantaneous bubble radius and time are non-dimensionalized as $R(t)/R(t_0)$ and t^*/τ_{eval}, where $\tau_{eval} \approx 0.91R(t_0)\sqrt{m\rho_l/P_\infty}$ is the approximated collapse time from the RP equation by neglecting surface tension and viscosity [35]. It is shown that both the DPD result and MD result have a similar trend and have little deviation from the RP equation lines, which may be caused by the fact that the parameters are not constant both in DPD and MD simulations. While the difference between the DPD result and the MD result is due to the effects of viscosity and surface tension, which have not been non-dimensionalized in τ_{eval}.

For the study on gaseous bubble oscillation, the quantitative comparison results are shown in fig. 6. The outside liquid pressure is increased from 1.30 to 11.35 to activate the bubble oscillation. Two typical cases are presented here with $r_C = 1.6$ (low density ratio of gas to liquid) and $r_C = 1.0$ (high density ratio) for bubble particles in DPD simulation, respectively, and the corresponding RP equation results are shown as smooth solid lines. The bubble radii from DPD simulation are derived from the instantaneous radial distribution function of the density of bubble particles. For both cases, the DPD results give consistent results of final stable bubble radii ($t^* > 40$) with RP equation results, whereas discrepancies are found for the oscillating frequencies of bubble radius, *i.e.*, the oscillating frequencies from DPD simulation are lower than the results from RP equations, which might be caused by the finite inertial and finite viscosity of bubble phase. As the r_C of bubble particles increases (from 1.0 to 1.6), the density ratio of gas to liquid decreases, and the result is getting closer to the results of the RP equation, which indicates us that the density ratio effect may not play a significant role in bubble oscillation when it ranges from 0.1 to 0. Moreover, on the other hand, the fluctuation nature in microscopic is well captured by our microbubble model.

Conclusion. – Studies on microbubble dynamics play an important role in hydrodynamics, biomedical engineering, etc. A microbubble model has been developed in the current work with the mesoscopic simulation tool, dissipative particle dynamics (DPD) and many-body dissipative particle dynamics (MDPD). The standard DPD particles are used to construct the bubble/gas

phase, whereas the MDPD particles are for the liquid phase. The current microbubble model benefits from the advantages of both DPD and MDPD. The microbubble can be stably sustained in contrast to the previous vacuum bubble model. A gas-liquid interface is created with density and pressure jumps across the interface. By varying the magnitudes of the cut-off radius and the conservative amplitude of bubble particles, the density ratio of gas to liquid can be lower than 0.1. The oscillating behavior the microbubble model is investigated by increasing the outside liquid pressure, the current model shows a correct dynamic response by comparing with the Rayleigh-Plesset equation from continuum theory, and the fluctuating behavior is captured as well. The lower the density ratio of the microbubble model, the closer the oscillating frequency to that of continuum theory, in which the inertial effect of bubble phase is neglected. This microbubble model in mesoscale is computationally efficient and moreover yields correct hydrodynamic behaviour. It is promising to apply the current model to the study of a large and complex system.

* * *

The authors are also grateful to the supports of the National Natural Science Foundations of China (Grant Nos. 11402230 and 91634103).

REFERENCES

[1] Ball P., *ChemPhysChem*, **13** (2012) 2173.
[2] Mørch K. A., *Interface Focus*, **5** (2015) 20150006.
[3] Ferrara K., Pollard R. and Borden M., *Annu. Rev. Biomed. Eng.*, **9** (2007) 415.
[4] Coussios C. C. and Roy R. A., *Annu. Rev. Fluid Mech.*, **40** (2008) 395.
[5] Choi J., Hsiao C. T., Chahine G. and Ceccio S., *J. Fluid Mech.*, **624** (2009) 255.
[6] Plesset M. S. and Prosperetti A., *Annu. Rev. Fluid Mech.*, **9** (1977) 145.
[7] Andersen A. and Mørch K. A., *J. Fluid Mech.*, **771** (2015) 424.
[8] Lohse D. and Zhang X. H., *Rev. Mod. Phys.*, **87** (2015) 981.
[9] Weijs J. H. and Lohse D., *Phys. Rev. Lett.*, **110** (2013) 054501.
[10] Hoogerbrugge P. and Koelman J., *EPL*, **19** (1992) 155.
[11] Español P. and Warren P., *EPL*, **30** (1995) 191.
[12] Pagonabarraga I. and Frenkel D., *J. Chem. Phys.*, **115** (2001) 5015.
[13] Warren P. B., *Phys. Rev. E*, **68** (2003) 066702.
[14] Trofimov S., Nies E. and Michels M., *J. Chem. Phys.*, **117** (2002) 9383.
[15] Groot R. D. and Warren P. B., *J. Chem. Phys.*, **107** (1997) 4423.
[16] Okumura H. and Ito N., *Phys. Rev. E*, **67** (2003) 045301.
[17] Fu H. H., Comer J., Cai W. S. and Chipot C., *J. Phys. Chem. Lett.*, **6** (2015) 413.
[18] Tran-Duc T., Phan-Thien N. and Khoo B. C., *J. Rheol.*, **57** (2013) 1715.
[19] Pan W., Pivkin I. V. and Karniadakis G. E., *EPL*, **84** (2008) 10012.
[20] Clark A. T., Lal M., Ruddock J. N. and Warren P. B., *Langmuir*, **16** (2000) 6342.
[21] Pan D., Phan-Thien N. and Khoo B. C., *J. Non-Newtonian Fluid Mech.*, **212** (2014) 63.
[22] Mai-Duy N., Pan D., Phan-Thien N. and Khoo B. C., *J. Rheol.*, **57** (2013) 585.
[23] Lin Y., Pan D., Li J., Zhang L. and Shao X., *J. Chem. Phys.*, **146** (2017) 124108.
[24] Yaghoubi S., Shirani E., Pishevar A. R. and Afshar Y., *EPL*, **110** (2015) 24002.
[25] Ghoufi A. and Malfreyt P., *Phys. Rev. E*, **83** (2011) 051601.
[26] Ghoufi A. and Malfrey P., *J. Chem. Theory Comput.*, **8** (2012) 787.
[27] Pan D., Phan-Thien N. and Khoo B. C., *Mol. Simul.*, **41** (2015) 1166.
[28] Caupin F., Arvengas A., Davitt K., Azouzi M. E. M., Shmulovich K. I., Ramboz C., Sessoms D. A. and Stroock A. D., *J. Phys.: Condens. Matter*, **24** (2012) 284110.
[29] Xiao C., Heyes D. and Powles J., *Phys. Status Solidi (b)*, **242** (2005) 749.
[30] Marmottant P. and Hilgenfeldt S., *Nature*, **423** (2003) 153.
[31] Rayleigh O. M., *Philos. Mag.*, **34** (1917) 94.
[32] Plesset M. S. and Chapman R. B., *J. Fluid Mech.*, **47** (1971) 283.
[33] Hołyst R., Litniewski M. and Garstecki P., *Phys. Rev. E*, **82** (2010) 066309.
[34] Hołyst R., Litniewski M. and Garstecki P., *Phys. Rev. E*, **85** (2012) 056303.
[35] Brennen C. E., *Cavitation and Bubble Dynamics* (Cambridge University Press) 2013.